Benha Veterinary Medical Journal 47 (2024) 40-47

Official Journal Issued by Faculty of Veterinary Medicine

Benha Veterinary Medical Journal

Journal homepage: https://bvmj.journals.ekb.eg/

Since 1990

Original Paper

Investigating the preventative and therapeutic effects of silver nanoparticles and zinc oxide quantum dots on *E. coli*- caused hepatorenal lesions in broiler chicks

Mohammed Abdeldayem M.A[1], Shawky A. Moustafa[1], Aziza A. Amin[1], Sawsan S. Elbasuni[2], Mohamed M.S. Gaballa[1*]

[1]*Department of Pathology, Faculty of Veterinary Medicine, Benha University, Benha 13726, Egypt.*

[2]*Department of Avian and Rabbit Diseases, Faculty of Veterinary Medicine, Benha University, Benha 13726, Egypt*

ARTICLE INFO

Keywords

E. coli

Nanoparticles

Poultry

Silver

Zinc oxide

Received 26/09/2024
Accepted 24/10/2024
Available On-Line 31/12/2024

ABSTRACT

Escherichia coli causes a significant threat to poultry, particularly with the rise of antibiotic resistance. This study investigated the protective and therapeutic efficacy of silver nanoparticles (Ag NPs) and zinc oxide quantum dots (ZnO QDs) in mitigating *E. coli*-induced hepatorenal lesions in broiler chicks. Eighty specific pathogen-free broiler chicks were divided into eight groups, including negative and positive controls, and preventive and therapeutic nanoparticle protocols. On Day 14, chicks were challenged with 1×10^8 CFU/ml of *E. coli* O78, and either Ag NPs (0.5 mg/kg) and ZnO QDs (80 mg/kg) was administered orally before (prevented groups, from day 8 to day 22) or after (treated groups, from day 16 to day 22) induction of infection. Histopathological scoring, morphometric analysis of inflammatory areas, and biochemical assays were used to assess tissue damage and organ function. Histopathological examination revealed severe hepatorenal lesions in the *E. coli*-infected group, including multifocal necrosis, hydropic degeneration, and inflammatory infiltration. Tubular epithelial degeneration and nephritis were prominent in the kidneys. Histopathological scoring declared that chicks treated with Ag NPs and ZnO QDs showed significantly reduced lesion severity. Inflammatory areas in the liver and kidneys were markedly diminished in the treated groups compared to the infected control. Biochemical analyses supported these findings, showing improved liver enzymes, creatinine, and uric acid levels, indicating liver and kidney functions restoration, and suggesting potent protective or therapeutic effects. In conclusion, Ag NPs and ZnO QDs significantly mitigated *E. coli*-induced hepatorenal damage and offered a promising alternative to traditional antibiotics in poultry.

1. INTRODUCTION

Escherichia coli infections in poultry, particularly in chicks, present a significant challenge in both veterinary and human public health sectors. Escherichia coli, a common gut inhabitant, can cause severe extraintestinal diseases, leading to high mortality rates and substantial economic losses in the poultry industry (Joseph et al., 2023). Avian pathogenic *E. coli* is manifested in localized infections such as yolk sac infection, peritonitis, salpingitis, and cellulitis, or systemic infections such as coli-septicemia, pericarditis, air-sacculitis, coli-granuloma, and arthritis (Panth, 2019). Among the various health complications, hepatorenal lesions are of particular concern due to their critical role in detoxification and metabolic processes in birds (Joshua et al., 2022). These lesions often result in reduced growth rates, poor feed conversion, and increased susceptibility to other diseases (Nolan et al., 2020). The pathogenesis of these lesions involves bacterial invasion and the subsequent inflammatory response, often leading to tissue damage and organ failure (Hu et al., 2022). Current treatment strategies largely rely on antibiotics; however, their overuse has led to the emergence of antibiotic-resistant *E. coli* strains, rendering this approach increasingly ineffective and calling for novel therapeutic strategies (Wibisono et al., 2022; Islam et al., 2023).

In the face of growing antibiotic resistance, there is an urgent need for alternative treatment strategies (Koutsianos et al., 2021). Nanotechnology offers promising solutions, especially in the development of nanomaterials with antimicrobial properties (Hetta et al., 2023). Among these, nano-silver has gained significant attention. Its mechanism of action involves the release of silver ions, which interact with bacterial cell membranes and intracellular structures, leading to cell death (Yin et al., 2020). Furthermore, nano-silver has been shown to disrupt bacterial DNA replication and promote oxidative stress within bacterial cells, making it a potent antibacterial agent (Ahmad et al., 2020).

Zinc oxide quantum dots (ZnO QDs) have also emerged as a novel antimicrobial agent. Their unique size-dependent properties, such as a high surface-to-volume ratio and quantum confinement effects, enable effective interactions with microbial cells (Li et al., 2021). Zinc oxide has been reported to exert antibacterial activity through the generation of reactive oxygen species (ROS), which induce oxidative stress and lead to bacterial cell damage (Khan et al., 2024). Additionally, ZnO QDs can disrupt bacterial cell membrane integrity and interfere with nutrient uptake,

* Correspondence to: Mohamed.gaballah@fvtm.bu.edu.eg

further enhancing their antimicrobial efficacy (Gangadoo et al., 2021; Gudkov et al., 2021).

The integration of nano-silver and zinc oxide quantum dots into veterinary medicine, specifically for the treatment and control of bacterial diseases in chicks, represents a cutting-edge approach. However, *In vivo* studies on these nanoparticles for *E. coli* prevention and treatment are limited. Therefore, this research focuses on exploring the protective and therapeutic potential of nano-silver and zinc oxide quantum dots against *E. coli*-induced hepatorenal lesions in chicks.

2. MATERIAL AND METHODS

2.1. Preparation of Silver nanoparticles (Ag NPs)

Silver nanoparticles were synthesized by reducing silver nitrate with chitosan. In a typical preparation, a solution of chitosan (6.92 mg/mL) was mixed with silver nitrate (52.0 mM) and stirred until homogenous. This mixture was then incubated for 12 hours at 95 °C, resulting in a color change from colorless to yellowish-brown, indicating the formation of silver nanoparticles. The resultant solution was directly used for antibacterial activity assessments. This method highlights the utilization of chitosan not only as a stabilizer but also as a reducing agent, facilitating the eco-friendly synthesis of silver nanoparticles with potent antibacterial properties (Wei et al., 2009).

2.2. Preparation of Zinc oxide quantum dots (ZnO QDs)

Zinc oxide quantum dots were synthesized using a sol-gel method. Initially, 0.03 mol of zinc acetate was dissolved in 0.15 liters of absolute ethanol and stirred for 30 minutes at 78 °C to create the precursor solution. Following this, 0.05 mol of KOH was dissolved in 0.03 liters of absolute ethanol and then added to the precursor solution, with the resultant mixture being stirred for 5 minutes. Next, 720 µl of APTES (3-Aminopropyltriethoxysilane) was diluted to 3.6 ml with ultrapure water and added dropwise to the mixture as a surface modifier. This mixture was then stirred for an additional ten minutes. Subsequently, it was centrifuged at 3500 rpm for 5 minutes and washed three times with absolute ethanol. Finally, the prepared sols were dried in an oven for 12 hours at 60 °C to yield the ZnO quantum dots (Li et al., 2021).

2.3. Characterization of the synthesized nanoparticles

The characterization of the synthesized nanoparticles includes the assessment of their optical properties and the determination of their size and shape. The UV-Vis absorption spectra of the nanoparticles were obtained using a V-730 UV-Vis spectrophotometer from Jasco. This instrumental analysis was crucial for determining the optical properties of the nanoparticles, which is an important aspect of their potential applications. Additionally, an XRD (X-ray diffraction) pattern was obtained using an XPERT-PRO Powder Diffractometer system, with a 2 Theta (20^{O} - 80^{O}), a minimum step size of 0.001, and a wavelength (Kα) = 1.54614^{O}. This analysis was crucial for understanding the crystalline structure of the quantum dots. The size and shape of the synthesized nanoparticles were characterized using Transmission Electron Microscopy (TEM). The TEM images were acquired using a JEOL JEM-2100 high-resolution transmission electron microscope (Shamhari et al., 2018).

2.4. Bacterial strain isolation, identification, and counting

Avian pathogenic *E. coli* isolate was obtained from the Bank of Bacterial strains, Animal Health Research Institute (AHRI), Cairo, Egypt. The strain was previously isolated from cases of coli-septicemia with high mortalities in broiler chicks, identified, and serotyped *E. coli* O78 (Ibrahim et al., 2024). *E. coli* O78 serotype was grown aerobically in nutrient broth at 37◦C for 24 h before using as a target organism. The dose was calculated to match 1×10^8 CFU/ml of bacterial isolate.

2.5. Ethical approval

The research was approved by the Scientific Research Ethical Committee, the Faculty of Veterinary Medicine, Benha University, under ethical approval number BUFVTM 08-01-24.

2.6. Experimental design

A total of 80- one-day-old specific pathogen-free (SPF) broiler chicks were purchased from Nile S.P.F Company, Faiyum, Egypt. The birds were reared in a building under controlled environmental conditions. The birds received *ad libitum* drinking water and feed mixtures according to the nutrient requirements of broilers. After an acclimatization period of one week, chicks were randomly divided into 8 groups (n=10/group). The control group was kept as a control non-infected group. Ag NPs group (silver nanoparticles group) received oral administration of Ag NPs only at a dose of 0.5 mg/kg body weight (bw) daily from 8^{th} to 22^{nd} day of age, as described by Hassanen et al. (2021). ZnO QDs group (zinc oxide quantum dots group) received oral administration of ZnO QDs only at a dose of 80 mg/kg body weight (bw) daily from 8^{th} to 22^{nd} day of age, as described by Li et al. (2021). E. *coli* group was challenged on 14^{th} day of age by crop gavage with 1×10^8 CFU/ml/bird of *E. coli* O78 in PBS according to the method described by (Abd El-Tawab et al., 2015). Ag NPs prevented group received 0.5 mg/kg bw Ag NPs daily from 8^{th} – 22^{nd} day of age and challenged at 14^{th} day of age. ZnO QDs prevented group received 80 mg/kg bw ZnO QDs daily from 8^{th} – 22^{nd} day of age and challenged at 14^{th} day of age. Ag NPs treated group was challenged at 14^{th} day of age and treated by 0.5 mg/kg bw Ag NPs daily from 16^{th} – 22^{nd} day of age (Hassanen et al., 2021; Zaoui et al., 2024). ZnO QDs treated group was challenged at 14^{th} day of age and treated by 80 mg/kg bw ZnO QDs daily from 16^{th} – 22^{nd} day of age (Hussien et al., 2021; Shi et al., 2024). All birds were monitored for clinical signs and mortality all over the experimental period.

2.7. Sampling, and necropsy findings

Blood samples were collected aseptically from the wing vein at the end of the experiment. Necropsy was conducted on each group at 19^{th} (n=5) and 22^{nd} (n=5) day of age to observe the gross lesions of the liver and kidneys. Tissue Specimens were collected from the liver and kidneys of sacrificed chicks for bacterial re-isolation and histopathological examination.

2.8. Serum biochemical assays

Serum was subsequently obtained through blood centrifugation for 10 minutes at 2000 g. The collected serum samples were then stored at -20°C until further analysis. To evaluate liver and kidney function, serum levels of aspartate aminotransferase (AST), alanine transaminase (ALT) were measured as described by (Reitman and Frankel, 1957; Szasz, 1969), and also uric acid and creatinine levels were evaluated according to (Caraway, 1963; Di Giorgio, 1974). All measurements were conducted using the Clinical Chemistry Analyzer SBA 733 Plus (Sunostik Medical Technology Co., Ltd, China).

2.9. Bacterial re-isolation

The blood and organ (liver and kidney) tissue homogenates were incubated aerobically in nutrient broth at 37◦C for 24 h before plotting on EMB agar. The isolated colonies were identified and serotyped according to the method described by Ibrahim et al. (2024).

2.10. Histopathological examinations

Tissue specimens from the liver and kidney were preserved in 10% neutral buffered formalin, dehydrated in ascending order of ethanol, cleared in xylene, paraffin-embedded, sliced with a microtome (5 µm), and stained with hematoxylin and eosin (H&E) for detection of histopathological alterations (Bancroft and Layton, 2019). Lesions in the hepatic and renal tissues were assessed using nominal and ordinal scoring methods. The nominal scoring system categorized lesions as either present or absent (Gibson-Corley et al., 2013), while the ordinal scoring system used a scale from 0 to 3, with 0 indicating no lesions, 1 representing mild lesions, 2 indicating moderate lesions, and 3 indicating severe lesions (Landmann et al., 2021). The ImageJ software version 1.48 was used to quantify the extent of inflammation in digital image analysis. This involved enhancing the blue color channel and adjusting thresholds to minimize background noise, allowing the software to isolate the nuclei of inflammatory cells in the histological images. The inflammatory area was then measured as a percentage of the total tissue area in each image, with five representative images analyzed per bird in each experimental group. The average inflammatory area was calculated by determining the mean percentage across all five images. The Lesion Detection Frequency (%) was calculated using the formula: (Number of Samples with Lesion / Total Number of Samples) × 100. The Average Score was calculated using the formula: ((N0 × 0) + (N1 × 1) + (N2 × 2) + (N3 × 3) / T, where N0 is the number of samples with no lesions (score 0), N1 is the number of samples with mild lesions (score 1), N2 is the number of samples with moderate lesions (score 2), N3 is the number of samples with severe lesions (score 3), and T is the total number of samples. The Average Inflammatory Area (%) was calculated by summing the percentages of the inflammatory areas and dividing by the number of images.

2.11. Statistical analysis

Data of serum biochemical liver and kidney functions were analyzed using one-way ANOVA followed by Tukey's multiple comparison test as post hoc test, with $p< 0.05$ considered statistically significant. Results are expressed as mean ± SD.

4. RESULTS

3.1 Synthesis and Characterization of Silver Nanoparticles

The typical UV–vis absorption spectra of the resulting solution display the characteristic surface plasmon resonance (SPR) band of silver nanoparticles centered at about 405 nm (Fig. 1A). The TEM images show the size and shape of the nanoparticles. The particles appear to be uniformly distributed with a spherical shape, which is consistent with the reported average size of 12 ±2 nm (Fig. 1B). The Selected Area Electron Diffraction (SAED) image (Fig. 1C) reveals the crystalline nature of the nanoparticles. The distinct spots in the SAED pattern indicate that the silver nanoparticles have a well-defined crystalline structure, which is important for their stability and functional properties.

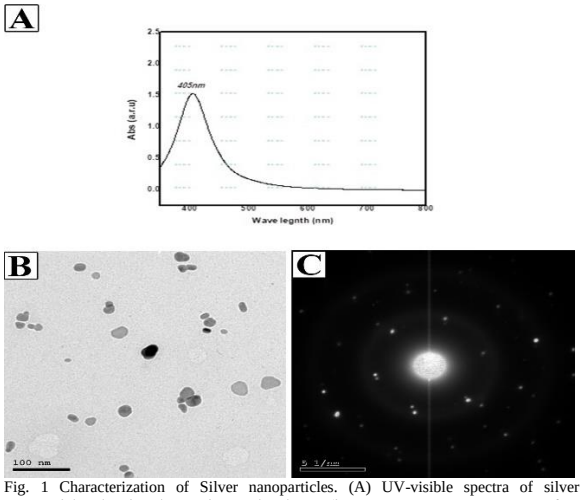

Fig. 1 Characterization of Silver nanoparticles. (A) UV-visible spectra of silver nanoparticles showing the maximum absorbance (λmax) at around 405 nm, the surface plasmon resonance of silver nanoparticles (B) TEM image of the silver nanoparticles. (C) SAED pattern of silver nanoparticles have a well-defined crystalline structure.

3.2 Characterization of Zinc oxide quantum dots

The X-ray diffraction (XRD) analysis revealed a clear diffraction pattern with sharp peaks, indicating that the prepared zinc oxide had a well-ordered crystalline structure (Fig. 2A), it also suggested that the sample is pure and did not contain crystalline impurities from other materials. The TEM images show the size and shape of the nanoparticles. The nanoparticles appear to have an approximately spherical shape with an average size of 10±2 nm, indicating that they are very small and within the nanometer range. (Fig. 2B). The SAED image (Fig. 2C) displayed the concentric ring pattern, suggesting that the material had a polycrystalline structure, meaning the nanoparticles consist of many small crystals.

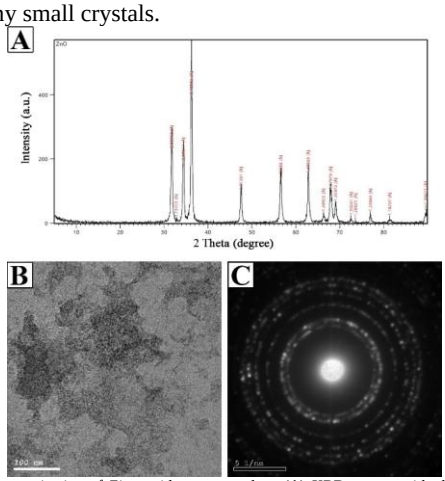

Fig 2 Characterization of Zinc oxide quantum dots. (A) XRD pattern with sharp peaks and a well-ordered crystalline structure. (B) TEM image of the ZnO QDs. (C) SAED pattern of ZnO QDs have a well-defined crystalline structure.

3.3 Clinical signs and gross lesions

Clinical features of E. coli group include lethargy, anorexia, ruffled feathers, gasping, and brown diarrhea. On necropsy, hepatomegaly, liver and kidney congestion with mild fibrinous layer, and hemorrhages were occasionally evident on the liver surface. Interestingly, these symptoms and lesions were mild in other treated groups and not detected in the control group.

3.4 Serum biochemistry

The E. *coli* group showed significant ($p< 0.0001$) increases in the liver (ALT and AST) and kidney function (uric acid and creatinine) values compared to the control group meanwhile, Ag NPs prevented or treated groups showed a

significant reduction ($p< 0.0001$) in the liver and ($p<0.001$) in kidney function biomarkers compared to *E. coli* group. Similarly, ZnO QDs prevented or treated groups showed a significant decrease in the liver ($p<0.0001$) and kidney function tests, uric acid ($p<0.01$), and creatinine ($p<0.05$) (Fig.3).

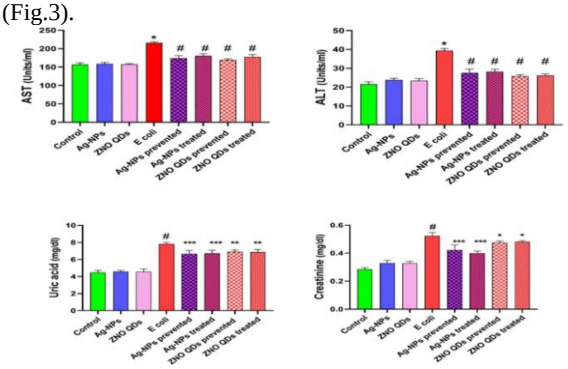

Fig. 3 Effects of *E. coli*, Ag NPs, and ZnO QDs on liver and kidney functions in each experimental group. Data was analyzed by one-way ANOVA followed by Tukey's multiple comparison test and $p < 0.05$ was statistically significant. In the liver, * P< 0.0001 compared with control; # P< 0.0001 compared with *E. coli* group. In kidney, # P< 0.0001 compared to control; ***P< 0.001; ** P<0.01; * P<.05 compared to *E. coli* group.

3.5 Microscopic Examination

3.5.1 Histopathological Examination

Histopathological analysis of liver and kidney tissues across various experimental groups demonstrated apparent differences in microscopic lesions. In the following groups: Control, Ag NPs, and ZnO QDs, at 19 days (Fig. 4 A-C) and 22 days (Fig. 4 G-I) sacrifices, the liver tissues exhibited minimal pathological alterations and preserved structural integrity. Hepatic lobules, central veins, and hepatocytes were well-organized, with hepatocytes presenting clear cytoplasm and distinct nuclei and no significant inflammatory response. Mild congestion and sinusoidal dilation were occasionally noted in the Ag NPs group (Fig. 4 B and H), while the ZnO QDs group displayed minor sinusoidal dilation, particularly at the second sacrifice (Fig. 4I); however, these changes did not compromise the overall liver architecture. In contrast, the *E. coli* group showed substantial liver damage at both 2 points (Fig. 4 D-F and J-L). This group exhibited extensive necrosis, pronounced hydropic degeneration, and substantial inflammatory cell infiltration. Hepatocytes adjacent to necrotic zones displayed severe swelling and vacuolation, with these areas densely infiltrated by inflammatory cells forming large nodular aggregates, most prominent at the second sacrifice. Additionally, bile ducts in the *E. coli* group showed mild proliferation and periductal fibrosis.

Among the hepatic lesions, lymphocytic cell aggregation was notably severe in the *E. coli* group, whereas the silver and zinc oxide nanoparticle-treated groups exhibited significantly less severe pathology (Fig. 5 A-H). The Ag NPs prevented, and Ag NPs treated groups demonstrated improvements (Fig. 5 A-D), showing reduced hydropic degeneration and vacuolation, with liver architecture largely preserved and less severe lymphocytic cell aggregation compared to the *E. coli* group. Similarly, the ZnO QDs prevented and ZnO QDs treated groups maintained a well-preserved liver structure with only mild vacuolation and minimal inflammation (Fig. 5 E-H).

At both sacrifice points, the kidney tissues of the Control, Ag NPs, and ZnO QDs groups maintained normal histological architecture. At the first sacrifice (Fig. 6 A-C) and the second sacrifice (Fig. 6 G-I), glomeruli were intact with well-defined Bowman's capsules, and there was no significant expansion of the mesangial matrix. Renal tubules were structurally sound, with clear cuboidal epithelial cells and no notable luminal debris. Mild degeneration was occasionally observed in the Ag NPs group (Fig. 6 B and H), and slight tubular epithelial swelling was noted in the ZnO QDs group at both sacrifices (Fig. 6 C and I), though these changes did not affect the overall renal architecture.

In contrast, the *E. coli* group exhibited severe kidney damage at both sacrifices. Glomeruli displayed significant injury and inflammatory cell infiltration. Renal tubules showed widespread degeneration, with swollen, vacuolated epithelial cells filled with eosinophilic debris, along with extensive tubular necrosis, particularly pronounced at the second sacrifice. Additionally, the renal interstitium was markedly expanded due to edema and infiltrated by lymphocytes.

The Ag NPs prevented, and Ag NPs treated groups showed notable improvements in renal health with reduced pathological changes. Compared to the *E. coli* group, there were fewer instances of tubular degeneration and vacuolation, and the kidney structure was better preserved (Fig. 7 A-D). Similarly, the ZnO QDs prevented and ZnO QDs treated groups exhibited well-preserved renal architecture with minimal vacuolation and inflammatory infiltration (Fig. 7 E-H). *3.5.2*

Histopathological Evaluation

The histopathological scoring and morphometric analysis showed different tissue damage and recovery patterns among the groups. The *E. coli* group had the most severe damage, while the control group had minimal changes. The silver and zinc oxide preventive and therapeutic groups showed varying degrees of improvement. Table (1) details the comparison of lesion detection frequency, severity scores, and inflammatory areas in liver and kidney tissues across all groups on the 19th and 22nd days.

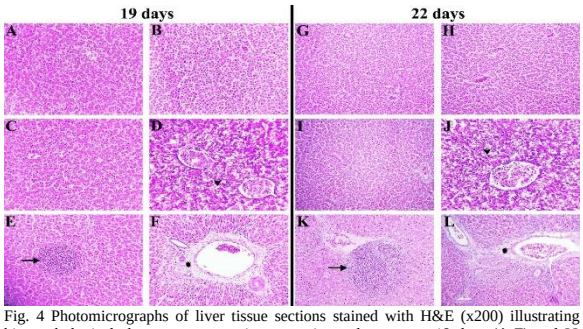

Fig. 4 Photomicrographs of liver tissue sections stained with H&E (x200) illustrating histopathological changes across various experimental groups at 19 days (A-F) and 22 days (G-L). The control, Ag NPs, and ZnO QDs groups demonstrated normal histological architecture at both time points (A-C and G-I). However, the Ag NPs group exhibiting mild congestion and sinusoidal dilation (B and H), while the ZnO QDs group displaying minimal sinusoidal dilation, particularly at the second sacrifice (I). The *E. coli* group, in contrast, showing severe pathological changes at both sacrifices, including significant congestion and vacuolation of hepatocytes (arrowheads) in (D and J), focal lymphocytic cell aggregation (arrows) in (E and K), and fibroblast activation with perivascular and periductal fibrosis (Asterisk) accompanied by inflammatory cell infiltration (F and L).

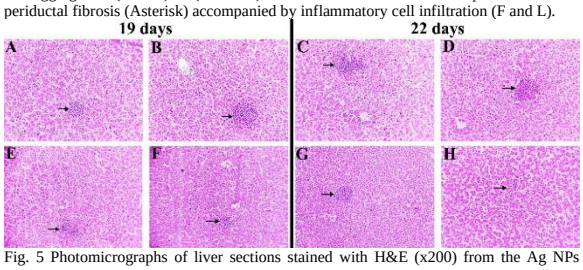

Fig. 5 Photomicrographs of liver sections stained with H&E (x200) from the Ag NPs prevented, Ag NPs treated groups at 19 days (A and B) and 22 days (C and D), and ZnO QDs prevented, and ZnO QDs treated groups at 19 days (E and F) and 22 days (G and H). The Ag NPs prevented, and Ag NPs treated groups improved liver pathology, especially lymphocytic cell aggregation (arrows) compared to the *E. coli* group, with reduced hydropic degeneration and preserved hepatic architecture (A-D). Similarly, the ZnO QDs prevented and ZnO QDs treated groups showed well-preserved liver structures with minimal vacuolation and inflammation (E-H), indicating effective prevention and treatment outcomes.

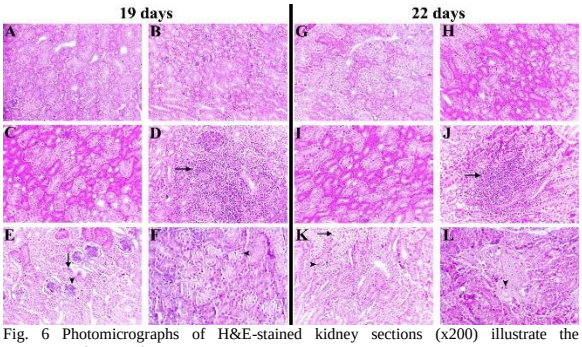

Fig. 6 Photomicrographs of H&E-stained kidney sections (x200) illustrate the histological findings for the Control, Ag NPs, ZnO QDs and *E. coli* groups at 19 days (A-F) and 22 days (G-L). The control group displayed a normal histological structure with well-preserved renal architecture (A and G). The Ag NPs group exhibited mild degeneration (B and H), while the ZnO QDs group showed slight degeneration (C and I); however, the overall renal structure remained intact in these groups. In contrast, the *E. coli* group demonstrated severe renal lesions at both sacrifices, including extensive inflammatory cell infiltration (arrows) between renal tubules (D and J), glomerular shrinkage (arrowheads) and degenerative changes in renal tubules (arrows) (E and K), and necrotic alterations such as eosinophilic cytoplasm and pyknotic nuclei (arrowheads) (F and L).

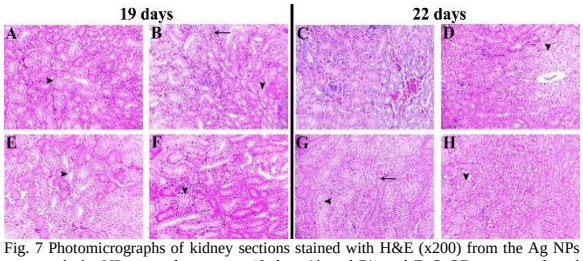

Fig. 7 Photomicrographs of kidney sections stained with H&E (x200) from the Ag NPs prevented, Ag NPs treated groups at 19 days (A and B), and ZnO QDs prevented, and ZnO QDs treated groups at 19 days (E and F) and 22 days (G and H). The Ag NPs prevented, and Ag NPs treated groups displayed reduced pathological changes, with fewer instances of tubular vacuolation (arrowheads), mild congestion, inflammatory cell infiltration (arrow) and preserved renal architecture (A-D). Similarly, the ZnO QDs prevented and ZnO QDs treated groups exhibited minimal vacuolation (arrowheads) and inflammation (arrow), indicating effective preventive and therapeutic effects on kidney tissue (E-H).

Table 1 Comparative histopathological evaluation of lesion detection frequency, severity and inflammation areas in liver and kidney tissues across experimental groups and sacrifice periods

Group	Sacrifice day	Lesion Detection Frequency in Liver	Average Score in Liver	Liver Inflammation Area Average (%)	Lesion Detection Frequency in Kidney	Average Score in Kidney	Kidney Inflammation Area Average (%)
Control	19th	10%	0.1	1.47	20%	0.2	0.712
	22nd	15%	0.15	1.84	20%	0.2	0.704
Indication	Minimal lesion detection frequency and very low average lesion scores with low inflammation area percentages. This indicates healthy tissue architecture and serves as a baseline for comparison.						
E. coli	19th	80%	2.3	7.96	90%	2.0	4.622
	22nd	85%	2.5	9.54	95%	2.3	4.16
Indication	The highest lesion detection frequency and greatest average lesion scores, with significantly elevated inflammation areas. This represents the maximum pathological state with severe tissue damage and inflammation.						
Ag NPs	19th	15%	0.15	1.59	30%	0.35	1.07
	22nd	25%	0.25	1.72	35%	0.4	1.08
Indication	Minimal pathological changes for assessing the effectiveness of silver nanoparticle treatment.						
Ag NPs prevented	19th	55%	0.9	2.55	60%	0.95	1.788
	22nd	45%	0.7	2.66	50%	0.75	1.8
Indication	Moderate lesion detection frequency and mild average lesion scores, with moderate inflammation areas. This indicates a preventive effect with a significant reduction in pathology compared to E. coli group.						
Ag NPs treated	19th	45%	0.8	2.47	40%	0.75	1.97
	22nd	35%	0.65	2.54	45%	0.85	1.84
Indication	Reduced lesion detection frequency and average lesion scores, with decreased inflammation areas. These results suggest effective treatment, showing better outcomes than prevention at the first sacrifice.						
ZnO QDs	19th	5%	0.05	1.13	10%	0.1	0.926
	22nd	5%	0.05	1.47	15%	0.15	0.984
Indication	Minimal pathological changes, even lower than control group, suggesting a potential protective effect.						
ZnO QDs prevented	19th	35%	0.5	2.66	45%	0.65	1.854
	22nd	40%	0.55	2.79	30%	0.35	1.886
Indication	Decreased lesion detection frequency and average lesion scores, with moderate inflammation areas. This suggests a preventive effect more effective than Ag NPs prevented group at the first sacrifice.						
ZnO QDs treated	19th	25%	0.25	2.58	30%	0.35	1.836
	22nd	30%	0.35	2.62	30%	0.4	1.79
Indication	Exhibited reduced lesion detection frequency and average lesion scores, with lower inflammation areas. These results indicate pronounced treatment effectiveness, surpassing the preventive effect.						

4. DISCUSSION

The growing resistance of bacterial strains to traditional antibiotics has driven the search for alternative antimicrobial solutions. In this regard, nanotechnology has emerged as a promising field, with different nanoparticles demonstrating potent broad-spectrum antimicrobial effects (Patra, 2019). The application of nanotechnology in poultry and animal nutrition offers considerable potential due to its distinct advantages. Notably, nanoparticles are more efficiently absorbed through the digestive tract compared to larger particles, enhancing their effectiveness (Swain et al.,2 021). Additionally, nano-additives can be easily incorporated into natural feed components, such as protein capsules, micelles, and other matrices, to augment their nutritional and therapeutic qualities (Gelaye, 2024). *Escherichia coli* infections represent a major issue in poultry due to their high morbidity and mortality, which result in significant economic losses (Kathayat et al,2 021). The pathogenesis of *E. coli*-induced hepatorenal lesions involves bacterial invasion followed by inflammatory responses, ultimately leading to tissue damage and organ dysfunction (Samudra et al., 2020). Therefore, this study aimed to assess the protective and therapeutic effects of silver nanoparticles (Ag NPs) and zinc oxide quantum dots (ZnO QDs) against E. *coli*-induced hepatorenal lesions in broiler chicks.

In the present study, the serum biochemical analysis of the *E. coli* group showed a significant increase in liver enzymes (ALT and AST), creatinine, and uric acid levels compared to the control group as previously recorded by (Sharma et al., 2015). Additionally, the rise in creatinine and uric acid levels may result from degenerative changes in the renal tubules, impairing the excretion of both uric acid and creatinine, and subsequently leading to their accumulation in the bloodstream (Kaneko, 1980). These findings were confirmed by the histopathological degenerative changes observed in both the liver and kidney. The administration of Ag NPs and ZnO QDs significantly enhanced liver and kidney function tests in treated broiler chicks. The serum levels of liver enzymes AST and ALT were markedly reduced in Ag NPs prevented, Ag NPs treated, ZnO QDs prevented, and ZnO QDs treated groups compared to the *E. coli* group, indicating reduced liver damage and improved hepatic function. These biochemical

findings were consistent with the histological observations, suggesting that the nanomaterials effectively alleviated liver injury and restored normal hepatic function (Hassanen and Ragab, 2021; Li et al., 2021). Similarly, kidney function tests demonstrated an improvement in creatinine and uric acid levels in all prevented and treated groups compared to the *E. coli* group. However, in contrast to the histological examination results, the ZnO QDs prevented and ZnO QDs treated groups exhibited less reduction in both creatinine and uric acid levels than the Ag NPs prevented, and Ag NPs treated groups. This inconsistency between histological and biochemical findings aligns with the results reported by (Hassan et al., 2021).

In the current study, *E. coli* group exhibited severe pathological changes in the liver and kidneys, including extensive multifocal areas of inflammation and necrosis, hydropic degeneration, vacuolation of hepatocytes, Kupffer cell hyperplasia, vascular congestion, and inflammatory nodule formation. These findings are in alignment with the results reported by Shah et al. (2019) and Sonwane et al. (2019). Additionally, the renal tissue displayed severe injury such as tubular epithelial degeneration and extensive interstitial inflammation. These findings are consistent with the observations of Hashem et al. (2022). These pathological changes could be attributed to the ability of hepatic and renal tissues to detoxify and eliminate enterotoxins produced by *E. coli* (Sonwane et al., 2019). Furthermore, *E. coli* infection triggers an inflammatory response, leading to the migration of leukocytes from the bloodstream to the site of infection. This leukocyte recruitment can be considered a hallmark of bacterial inflammation and represents a key aspect of the immune system's defense against *E. coli* invasion (Romero et al., 2015).

Both Ag NPs and ZnO QDs, administered in preventive and therapeutic regimens, mitigated the *E. coli*-induced hepatorenal lesions to varying degrees. Ag NPs prevented, and Ag NPs treated groups exhibited moderate to marked reductions in lesion detection frequency, lesion scores, and inflammation areas compared to the *E. coli* group, suggesting that Ag NPs have the potential to protect against and treat *E. coli*-induced tissue damage. The precise mechanisms of action of silver nanoparticles are not fully understood, but Bruna et al. (2021) identify and summarize the three most supported mechanisms of AgNPs' antibacterial action according to the literature, including membrane damage, intracellular disruption, and the release of silver ions. The third mechanism suggested to occur concurrently with the other two, involves silver ions whose size and electrical charge may induce bacterial cellular damage and dysfunction. Furthermore, the authors emphasize how the nanoparticles' properties—such as their chemical composition, size, charge, and surface characteristics-affect their antibacterial efficacy.

ZnO QDs prevented and ZnO QDs treated groups also demonstrated promising results, with the ZnO QDs treated group which showed the most pronounced therapeutic effect. The lesion detection frequency, lesion scores, and inflammation areas in the ZnO QDs treated group were significantly lower than those observed in the *E. coli* group and the Ag NPs prevented and Ag NPs treated groups. This superior performance of ZnO QDs can be attributed to their unique size-dependent properties, such as a high surface-to-volume ratio and quantum confinement effects, which enhance their antimicrobial activity. ZnO QDs exert their antibacterial effects through the generation of reactive oxygen species, disruption of cell membrane integrity, and interference with nutrient uptake (Li et al., 2021).

5. CONCLUSIONS

In conclusion, both Ag NPs and ZnO QDs demonstrated protective and therapeutic effects against *E. coli*-induced hepatorenal lesions in broiler chicks. ZnO QDs, particularly in therapeutic applications, exhibited superior efficacy. These findings suggest that nanoparticles could serve as a promising alternative to traditional antibiotics in poultry. However, further research is needed to better understand their mechanisms of action and determine the optimal concentrations and dosages of these nanoparticles for effective use in veterinary medicine.

6. REFERENCES

1. Abd El-Tawab, A.A., El-komy, A.A., El-Ekhnawy, K.I. and Talaie, A.T., 2015. Effect of fosfomycin on E. coli O78 isolated from broiler chickens in-vitro and in-vivo. Benha Vet. Med. J, 281, 294-300.
2. Ahmad, S.A., Das, S.S., Khatoon, A., Ansari, M.T., Afzal, M., Hasnain, M.S. and Nayak, A.K., 2020. Bactericidal activity of silver nanoparticles: A mechanistic review. Materials Science for Energy Technologies, 3, 756-769.
3. Bancroft, J.D., Layton, C., 2019a. The hematoxylin and eosin. In: Suvarna, S.K., Layton, C., Bancroft, J.D., Eds., Bancroft's Theory and Practice of Histological Techniques, 8th Ed. Elsevier, Philadelphia, 126–138.
4. Bruna, T., Maldonado-Bravo, F., Jara, P. and Caro, N., 2021. Silver nanoparticles and their antibacterial applications. International Journal of Molecular Sciences, 22,13, 7202. https://doi.org/10.3390/ijms22137202
5. Caraway, W. 1963. Standard methods of clinical chemistry. Academic, New York, London 4, 239. https://doi.org/10.1016/B978-1-4831-9685-5.50029-7
6. Di Giorgio, J. 1974. Nonprotein nitrogenous constituents. Clinical chemistry: principles and technics, Harper and Row, New York, 514-517.
7. Gangadoo, S., Xu, C., Cozzolino, D., Latham, K., Della Gaspera, E., Chapman, J. and Truong, V.K., 2022. Probing nanoscale interactions of antimicrobial zinc oxide quantum dots on bacterial and fungal cell surfaces. Advanced Materials Interfaces, 9,3,2101484.https://doi.org/10.1002/admi.202101484
8. Gelaye, Y., 2024. Application of nanotechnology in animal nutrition: Bibliographic review. Cogent Food & Agriculture, 10,1,2290308.https://doi.org/10.1080/23311932. 023.2290308
9. Gibson-Corley, K.N., Olivier, A.K., and Meyerholz, D.K. ,2013. Principles for valid histopathologic scoring in research. Veterinary Pathology, 50,6, 1007-1015. https://doi.org/10.1177/0300985813485099.
10. Gudkov, S.V., Burmistrov, D.E., Serov, D.A., Rebezov, M.B., Semenova, A.A. and Lisitsyn, A.B., 2021. A mini review of antibacterial properties of ZnO nanoparticles. Frontiers in Physics, 9, 641481. https://doi.org/10.3389/fphy.2021.641481
11. Hashem, M.A., Hassan, A.E., Abou-Elnaga, H.M., Abdo, W., Dahran, N., Alghamdi, A.H. and Elmahallawy, E.K., 2022. Modulatory effect of dietary probiotic and prebiotic supplementation on growth, immuno-biochemical alterations, DNA damage, and pathological changes in E. coli-infected broiler chicks. Frontiers in Veterinary Science, 9, 964738. https://doi.org/10.3389/fvets.2022.964738
12. Hassan, S.A., Mujahid, H., Ali, M.M., Irshad, S., Naseer, R., Saeed, S., Firyal, S. and Arooj, F., 2021. Synthesis, characterization and protective effect of green tea-mediated zinc oxide nanoparticles against ochratoxin A induced hepatotoxicity and nephrotoxicity in albino rats. Applied Nanoscience, 11,8, 2281-2289.
13. Hassanen, E.I., Morsy, E.A., Hussien, A.M., Farroh, K.Y. and Ali, M.E., 2021. Comparative assessment of the bactericidal effect of nanoparticles of copper oxide, silver, and chitosan-silver against Escherichia coli infection in broilers. Bioscience Reports, 41,4,BSR20204091.https://doi.org/10.1042/BSR20204091
14. Hassanen, E.I. and Ragab, E., 2021. In vivo and in vitro assessments of the antibacterial potential of chitosan-silver nanocomposite against methicillin-resistant Staphylococcus

aureus–induced infection in rats. Biological Trace Element Research, 199,1, 244-257.
15. Hetta, H.F., Ramadan, Y.N., Al-Harbi, A.I., A. Ahmed, E., Battah, B., Abd Ellah, N.H., Zanetti, S. and Donadu, M.G., 2023. Nanotechnology as a promising approach to combat multidrug resistant bacteria: a comprehensive review and future perspectives. Biomedicines, 11,2, p.413. https://doi.org/10.3390/biomedicines11020413
16. Hu, J., Afayibo, D.J.A., Zhang, B., Zhu, H., Yao, L., Guo, W., Wang, X., Wang, Z., Wang, D., Peng, H. and Tian, M., 2022. Characteristics, pathogenic mechanism, zoonotic potential, drug resistance, and prevention of avian pathogenic Escherichia coli, APEC. Frontiers in Microbiology, 13, p.1049391. https://doi.org/10.3389/fmicb.2022.1049391
17. Hussien, K.R.A., Ismail, Z.S.H. and Abdel-Wareth, A.A.A., 2021. Application of zinc oxide nanoparticles as feed additive in broiler chicken nutrition under hot environmental conditions. SVU-International Journal of Agricultural Sciences, 3,3, 159-169. 10.21608/svuijas.2021.80159.1116
18. Ibrahim, A.H., El Khashab, E., Shakal, M. and Morsy, E.A., 2024. Unveiling Antibiotic Resistance, Virulence, and Molecular Detection of Enteric Bacterial Infections in Broilers: A Study in Egypt. Egyptian Journal of Veterinary Sciences, 55,6, 1537-1551.
19. Islam, M.S., Hossain, M.J., Sobur, M.A., Punom, S.A., Rahman, A.T. and Rahman, M.T., 2023. A Systematic Review on the Occurrence of Antimicrobial-Resistant Escherichia coli in Poultry and Poultry Environments in Bangladesh between 2010 and 2021. BioMed Research International, 2023,1, 2425564. https://doi.org/10.1155/2023/2425564
20. Joseph, J., Zhang, L., Adhikari, P., Evans, J.D. and Ramachandran, R., 2023. Avian pathogenic Escherichia coli , APEC in broiler breeders: an overview. Pathogens, 12,11, 1280. https://doi.org/10.3390/pathogens12111280
21. Joshua, B.I., Nanchak, L.R., Ayo, A.C., Jummai, B.D., Emmanuel, L.L., Suleiman, I., Alesa, U.M., Dominic, U.A., Pwajok, C.T.P., Gunya, D.Y. and Elisha, I.L., 2022. Gross and histopathological lesions associated with Escherichia coli infection in chickens examined, at Ecwa Veterinary Clinic, Bukuru, Plateau State, Nigeria. Acta Scientific Microbiology, 5, 74-81.
22. Kaneko, J.J., 1980. Serum proteins and the dysproteinemias. In Clinical biochemistry of domestic animals, 97-118. Academic Press.
23. Kathayat, D., Lokesh, D., Ranjit, S. and Rajashekara, G., 2021. Avian pathogenic Escherichia coli, APEC: an overview of virulence and pathogenesis factors, zoonotic potential, and control strategies. Pathogens, 10,4, p.467. https://doi.org/10.3390/pathogens10040467
24. Khan, S.U., Eren, G.O., Atac, N., Onal, A., Qureshi, M.H., Cooper, F.K., Almammadov, T., Kolemen, S., Sahin, M., Can, F. and Nizamoglu, S., 2024. Antibacterial type-II InP/ZnO quantum dots via multimodal reactive oxygen species. Chemical Engineering Journal, 480, 148140. https://doi.org/10.1016/j.cej.2023.148140
25. Koutsianos, D., Athanasiou, L., Mossialos, D. and Koutoulis, K.C., 2020. Colibacillosis in poultry: A disease overview and the new perspectives for its control and prevention. Journal of the Hellenic Veterinary Medical Society, 71,4, 2425-2436.
26. Landmann, M., Scheibner, D., Graaf, A., Gischke, M., Koethe, S., Fatola, O.I., Raddatz, B., Mettenleiter, T.C., Beer, M., Grund, C. 2021. A Semiquantitative Scoring System for Histopathological and Immunohistochemical Assessment of Lesions and Tissue Tropism in Avian Influenza. Viruses, 13,5, 868. https://doi.org/10.3390/v13050868.
27. Li, Y., Xie, S., Xu, D., Shu, G. and Wang, X., 2021. Antibacterial activity of ZnO quantum dots and its protective effects of chicks infected with Salmonella pullorum. Nanotechnology, 32,50, 505104. 10.1088/1361-6528/ac2846
28. Nolan, L.K., Barnes, H.J., Vaillancourt, J.P., Abdul-Aziz, T. and Logue, C.M., 2013. Colibacillosis. Diseases of poultry,13th ed., 751-805. https://doi.org/10.1002/9781119421481.ch18
29. Panth, Yuvraj. 2019. "Colibacillosis in Poultry: A Review." Journal of Agriculture and Natural Resources 2 ,1: 301–311. https://doi.org/10.3126/janr.v2i1.26094.
30. Patra, A.K., 2019. Are nanomaterials potential new generation antimicrobial feed additives in livestock. Indian Journal of Animal Health, 58, 105-120.
31. Reitman, S. and Frankel, S. 1957. A colorimetric method for the determination of serum glutamic oxalacetic and glutamic pyruvic transaminases." American journal of clinical pathology 28,1, 56-63. https://doi.org/10.1093/ajcp/28.1.56
32. Romero, R.T., Dos Santos, T.S., De Mato, F.P., Franciosi, A., Campois, N.F., Sarmiento, J.P., Nakazato, G., Gualtieri, K.D. and Campois, T.G., 2015. Study of cell migration in intraperitoneal infection by Escherichia coli in Mice Swiss. In Front. Immunol. Conference Abstract: IMMUNOCOLOMBIA2015-11th Congress of the Latin American Association of Immunology-10o. Congreso de la Asociación Colombiana de Alergia, Asma e Inmunología. doi: 10.3389/conf. fimmu ,Vol. 24.
33. Saad, D.Y., Khalil, H.A., Farouk, A.E., Soliman, A.M. and Mohamed, A.S., 2023. Therapeutic Effect of Chitosan-Zinc Oxide Nanoparticles on Acute Kidney Injury Induced by Gentamicin in Wistar Rats. Current Nanomedicine, Formerly: Recent Patents on Nanomedicine, 13,3, 217-227.
34. Samudra, D., Santoso, S., Asmoro, A.A., Khotimah, H., Ansori, A.N. and Sabdoningrum, E.K., 2020. The effect of Escherichia coli on pro-inflammatory mediators level and kidney and liver function of sepsis in Rattus novergicus. Indian J Forensic Med Toxicol, 14, p.4302. https://doi.org/10.37506/ ijfmt.v14i4.12315
35. Shah, S.A., Mir, M.S., Wani, B.M., Kamil, S.A., Goswami, P., Amin, U., Shafi, M., Rather, M.A. and Beigh, A.B., 2019. Pathological studies on avian pathogenic Escherichia coli infection in broilers. Pharm. Innov. J, 8,7, 68-73.
36. Shamhari, N.M., Wee, B.S., Chin, S.F. and Kok, K.Y., 2018. Synthesis and Characterization of Zinc Oxide Nanoparticles with Small Particle Size Distribution. Acta Chimica Slovenica, 65,3. https://doi.org/10.17344/acsi.2018.4213
37. Sharma, V., Jakhar, K.K., Nehra, V. and Kumar, S., 2015. Biochemical studies in experimentally Escherichia coli infected broiler chicken supplemented with neem ,Azadirachta indica leaf extract. Veterinary world, 8,11, 1340. 10.14202/vetworld. 2015.1340-1345
38. Shi, L., Ruan, M.L., Zhang, B.B., Gong, G.X., Li, X.W., Refaie, A., Sun, L.H. and Deng, Z.C., 2024. Effects of dietary supplementation of zinc oxide quantum dots on growth performance and gut health in broilers. Biological Trace Element Research, 1-9. https://doi.org/10.1007/s12011-024-04371-6
39. Sonwane, S.R., Ingole, R.S., Hedau, M.S., Hajare, S.W. and Ingawale, M.V., 2019. The ameliorative effect of Andrographis paniculata on E. coli-induced pathology in broilers. Veterinarski arhiv, 89,4, 545-557.
40. Swain, P.S., Prusty, S., Rao, S.B.N., Rajendran, D. and Patra, A.K., 2021. Essential nanominerals and other nanomaterials in poultry nutrition and production. Advances in poultry nutrition research. 10.5772/intechopen.96013
41. Szasz, G., 1969. A kinetic photometric method for serum γ-glutamyl transpeptidase. Clinical chemistry, 15,2, 124-136.
42. Wei, D., Sun, W., Qian, W., Ye, Y. and Ma, X., 2009. The synthesis of chitosan-based silver nanoparticles and their antibacterial activity. Carbohydrate research, 344,17, 2375-2382.
43. Wibisono, F.J., Effendi, M.H. and Wibisono, F.M., 2022. Occurrence, antimicrobial resistance, and potential zoonosis risk of avian pathogenic Escherichia coli in Indonesia: a review. http://www.doi.org/10.14202/IJOH.2022.76-85
44. Yin, I.X., Zhang, J., Zhao, I.S., Mei, M.L., Li, Q. and Chu, C.H., 2020. The antibacterial mechanism of silver nanoparticles and its application in dentistry. International Journal of Nanomedicine,15, 2555-2562.
45. Zaoui, Y., Belanche, A., Ben-Jeddou, K., Jiménez, M.S., Fondevila, G. and Fondevila, M., 2024. Effect of the dietary administration pattern of silver nanoparticles on growth performance, biodiversity of digestive microbiota and tissue retention in broiler chickens. Animal Feed Science and Technology, 309, p.115888. https://doi.org/10.1016/j.anifeedsci.2024.115888